

Influence of Switching Frequency and Squirrel Cage Design on Audible Noise and Losses in Induction Motor Drives

S. Van Haute, A. Malfait, R. Belmans

Katholieke Universiteit Leuven
E.E. Dept, ESAT-ELEN
Kardinaal Mercierlaan 94
B-3001 Leuven, Belgium

Keywords : induction motor, PWM inverter, switching frequency, audible noise, drive losses.

Summary

A large number of experiments are performed to analyse the influence of the inverter type and the switching frequency on the audible noise, losses and overall efficiency in variable speed induction motor drives. Temperature measurements both in stator and rotor give an indication of the required derating, if any. Results for a standard design motor, consecutively supplied by a transistor based inverter and IGBT inverter are compared with the behaviour when the machine is directly connected to the mains (Figure 1). To analyse the influence of the rotor design, a special rotor with no current redistribution is constructed and mounted in a rewind stator. Higher switching frequencies have a large influence on audible noise and temperature, but the overall efficiency remains nearly constant. However, it is shown that the distribution of losses is influenced.

1. Introduction

The use of variable speed drives has gained increasing importance over the last years. For small and medium sized drives, PWM voltage source inverters are standard nowadays. The IGBT based inverters yield high switching frequencies and high power ratings. Power ratings up to several hundreds of kVA are available commercially. The switching frequency might be several kHz.

Manufacturers claim that the increased switching frequencies lead to lower losses than normally found in inverter supplied machines (Boglietti et al (1), Chalmers et al (2), Murphy et al (3), Tomita et al (4), Kirschen et al (5), Lajoie-Mazenc et al (6) and Malfait et al (7)). Therefore, derating the motor at rated speed would not be required. The information given is always put into very simple terms and no information is given on the type of load used or the design of the motor involved in the tests. No indications are found how pronounced the optimum switching frequency is and how it is determined.

Furthermore, the low harmonic content reduces audible noise problems as shown by Belmans et al (8-9-10). Due to the increased switching frequency, the harmonic content of the supplied voltages and currents is improved, leading to a diminished possibility of encountering resonance frequencies and thus high audible noise levels.

This paper describes a large number of experiments comparing losses, overall efficiency and audible noise in induction motor drives with different types of inverters and changing switching frequency. Temperature measurements both in stator and rotor give an indication of the required derating, if any.

2. Motor and inverter used for the experiments

Tests are performed on different motor and inverter combinations (Figure 1). The first motor used is a standard 13.5 kW machine with a double cage rotor. The rated speed is 1455 rpm. The double bar construction is a standard design by European manufacturers. The rotor bars are skewed and made in cast aluminium. These bars are not insulated with respect to the rotor iron leading to supplementary losses due to interbar currents. This type of rotor is required to increase the starting torque when supplying the motor directly from the mains (reference: SS motor, i.e. Standard stator; Standard rotor).

In order to introduce temperature sensors in the stator, it is rewound. The original double layer winding is substituted by a single layer winding (RS motor: Rewound stator; Standard rotor). Both at fan side and load side six platinum resistors (Pt-100) are introduced in the stator slots. They are placed equidistant along the stator circumference, resulting in 4 Pt-100 sensors per phase. In the original standard double cage rotor one Pt-100 sensor is mounted as well. The sensor is located between two bars at 5 cm from the rotor front edge (fan side). The rotor signal is transferred to the stator via a slip ring arrangement.

In the double cage rotor current redistribution produces the high starting torque when the motor is connected to the mains. In inverter supplied induction motors, these starting problems are not present and current redistribution merely leads to an increase of the losses due to the harmonics of the non sinusoidal voltage. In order to assess the influence of current redistribution, a special rotor is built (RR motor, Rewound stator; Reconstructed rotor). This rotor has insulated round copper bars in open slots. The number of rotor bars is kept the same and no skewing is applied. The cross section area of the bars is chosen in a way that the dc resistance is equal to the original standard rotor. A temperature sensor is located on the same spot. When mounted in the rewound stator, the motor is referred to as the RR motor.

Two types of inverters are used in the experiments. Both are voltage source inverters with Pulse Width Modulation (PWM). The first is transistor based and has a pre-set switching frequency. The second is an IGBT inverter with controllable switching frequency between 1 and 12 kHz. Unless otherwise mentioned, the tests are done in the normal operation mode, i.e. the Volts/Hertz ratio is kept constant. As a reference, all motors can be connected to a 50 Hz sinusoidal supply, since this yields the ultimate optimum regarding harmonic frequency content.

3. Measuring set-up

The induction motor is loaded with an eddy current brake that can be controlled accurately. The overall lay-out of the measuring set-up is shown on Figure 2.

The audible noise is measured in a semi-anechoic chamber, avoiding interference with the frequency inverter audible noise and reflections of the walls and other material near to the set-up. The load has a very low audible noise level due to special bearings and water cooling. Both the overall noise levels in dB_{lin} or dB(A), and its frequency spectrum are measured using a condenser microphone.

A torque transducer is used to couple both machines. The transducer contains strain gauges, linked with the stationary recording equipment using a frequency modulated transmitter system. These measurements yield a very high accuracy, far better than the reaction torque often used as an alternative. In the torque transducer a speed transducer is incorporated, yielding the mechanical power. The accuracy of the output power is better than 0.5 %.

For the assessment of the electrical power between inverter and motor, special attention has to be paid to the harmonics in both current and voltage. This excludes the use of standard power measuring equipment. The frequency spectrum of the power measuring equipment goes up to 200 kHz, accounting for the power transduced by the higher harmonics. The accuracy of the power between inverter and motor is 0.5 %.

All power measuring equipment is connected to a data acquisition system. Using Labview all measured data are visualised. The data are gathered sufficiently fast to avoid fluctuations of the operating point.

Even if the switching frequency can be controlled, as in the IGBT inverter, the inverter changes the operating switching frequency with respect to the pre-set and displayed value due to the internal logic circuit. Therefore, voltage and current spectra are monitored and recorded. From these spectra, the actual switching frequency can be determined. In tables and graphs below, the actual switching frequencies will be indicated.

4. Audible noise

Both the overall audible noise level and the noise spectrum are measured for each motor-supply combination and different loads. A selection of all the measurements is presented.

4.1. Overall audible noise level

As prescribed in the standards, a dB(A) filter is used. Table 1 shows the results at fundamental frequencies of 50 Hz and 30 Hz and a load torque of 60 Nm. The highest switching frequency reduces firmly the audible noise level. The difference relative to the mains supply is less than 1 dB(A). If a switching frequency of 1 kHz is used, (IGBT or transistor based inverter), the increase is more pronounced. The influence of switching frequency can be seen more clearly in figure 3, where the overall audible noise level at different fundamental frequencies is presented as a function of the switching frequency. The top graph shows the results for the standard motor (SS) loaded with 60 Nm torque and supplied by the IGBT inverter, while the bottom graph gives the results for rewound stator with the original rotor (RS).

TABLE 1 - Audible noise [dB(A)] of different motor-supply combinations at a load of 60 Nm and fundamental frequency of 50 Hz (top) and 30 Hz (bottom)

Motor	Mains Supply	IGBT-Inverter		Transistor Inverter
	Sinusoidal	1.2 kHz	12 kHz	1 kHz
SS	74.8	78.0	75.5	77.0
RS	68.8	71.5	69.4	74.6
RR	75.1	77.0	75.4	77.7

Motor	IGBT-Inverter		Transistor Inverter
	1 kHz	12 kHz	1 kHz
SS	75.2	69.6	75.0
RS	74.6	62.9	73.5

From these measurements, the following conclusions can be drawn.

- At a switching frequency of 3 kHz, the overall audible noise level is higher than expected in the case of fundamental frequencies up to 40 Hz. This is due to the excitation of a natural frequency of the stator by the frequency of one of the vibrations produced by the electromagnetic forces caused by the switching frequency. For the motor with double layer stator winding at higher frequencies these phenomena do not occur.
- In case of the modified stator, a higher level is also recognised at 50 Hz ($f_{\text{switch}} = 5.4 - 6 \text{ kHz}$) and at 40 Hz ($f_{\text{switch}} = 11 \text{ kHz}$). This is due to the occurrence of subharmonics in the voltage spectrum, as noticed in figure 6.
- Generally the overall audible noise level decreases when the switching frequency increases. Particularly up to 8 kHz and fundamental frequencies below 50 Hz, there is a large drop in the audible noise. Thus, at lower motor speeds the overall audible noise is strongly reduced by applying higher switching frequencies. Once the switching frequency is above 8 kHz, the overall audible noise level is stabilised.
- At higher fundamental frequencies respectively at higher motor speeds the overall audible noise level has a small decrease as the switching frequency increases: the audible noise of the fan dominates the overall audible noise level.
- If no resonance occurs between the forces caused by the space harmonics in the flux density distribution in the air gap, and the stator natural frequencies, the motor with the single layer stator winding produces less audible noise than the original motor. This is due to the more stiff type of insulation material used during rewinding: a higher class of insulation material is used, generally leading to a higher stiffness of the link between stator winding and stator iron as indicated by Verdyck et al (11,12).
- Considering the motor with the copper rotor, it can be stated that the audible noise level is higher than using the original rotor (table 1a and b), caused by the high number of slotting harmonics. The harmonics are due to fact that the new rotor has open rotor slots, while the original one has closed ones. Furthermore, the copper rotor is not skewed, again increasing the influence of the harmonics, and thus increasing the audible noise level.

4.2 Audible noise spectrum

All measurements are performed in dB without filtering the input signal of the microphone. Apart from the level as such, pure tones may be noticed in the spectra.

In order to show the influence of the frequency spectrum of the supplied voltage, the spectra of the audible noise are compared. As an example, figure 4 shows the frequency spectrum of the RS motor loaded with 75 Nm when supplied consecutively from the 50 Hz mains and the transistor inverter. In the inverter supply spectrum, a large number of pure tones is present. The high peak of 71 dB at about 1.1 kHz is caused by one of the sidebands in the voltage spectrum. Figure 5 shows the audible noise spectrum of the same motor at the same speed and load conditions, but supplied by the IGBT-inverter switching at 12 kHz. Thus, one could conclude that the frequency spectrum at high switching frequencies is improved a lot.

In some cases, however, strong subharmonics appear causing more pure tones. Figure 6 shows the voltage and noise spectrum for the same motor at a fundamental frequency of 40 Hz and a switching frequency of 11 kHz. Also the overall noise level increases, as noticed above (figure 3).

As the human ear is particularly sensitive to pure tones, the audible noise of inverter supplied machines containing such tones is found to be very disturbing. This problem may be cured by using random PWM techniques: rather than avoiding an increase of the overall level, they reduce the presence of audible noise components having pure tones.

5. Temperature, losses and efficiency

Unless otherwise mentioned all power measurements are carried out after reaching thermal equilibrium in the motor. In the RS and RR motor the temperature is measured using Pt-100 sensors both in rotor and stator. During the tests, the ambient temperature was kept between 22°C and 23°C.

In inverter supplied induction motor drives, special attention should be given to the definition of losses and efficiencies. The following definitions are used:

- Fundamental power:

$$P_{\text{fund}} = U_1 I_1 \cos \varphi_1 \quad (1)$$

- Harmonic losses:

$$P_{\text{harm}} = P_{\text{conv.out}} - P_{\text{fund}} = \sum_{i=2}^{\infty} U_i I_i \cos \varphi_i \quad (2)$$

- Motor losses:

$$P_{\text{motor}} = P_{\text{fund}} - P_{\text{mech}} \quad (3)$$

- Inverter losses:

$$P_{\text{conv}} = P_{\text{conv.in}} - P_{\text{conv.out}} \quad (4)$$

- Overall losses:

$$P_{\text{tot}} = P_{\text{mech}} - P_{\text{conv.in}} \quad (5)$$

- Overall drive efficiency:

$$\eta_{\text{tot}} = \frac{P_{\text{mech}}}{P_{\text{conv.in}}} \quad (6)$$

How to define motor and inverter efficiencies is a subject being discussed. Using the fundamental power between inverter and rotor is one possibility (7). However, only the losses and total drive efficiency are considered here. The latter quantity is the most important from the user point of view, as he is not interested as such in the actual distribution of the losses amongst the different components of the drive, except for the temperature distribution as discussed below.

5.1. Influence of motor design

The type of motor being used is very important. Motors experiencing a large amount of current redistribution in the rotor during sinusoidal supply cause extra losses with inverter supply as the high frequency currents are concentrated in the upper portion of the rotor bars. To analyse the influence of the rotor lay out, the RS and RR motor are compared.

Table 2 shows overall efficiencies at a fundamental frequency of 50 Hz and a load torque of 75 Nm. Other tests are done at fundamental frequencies of 30 Hz and a load of 60 Nm. During these tests, the temperature is measured. Table 3 shows the results for stator (top) and rotor (bottom). It should be stressed that these temperatures are not the maximum values occurring in the motor. They only give an indication of the relative temperature rise of the different motors. The stator temperature is the average of the six temperature sensors on the load side of the motor. In both rotors the temperature sensor is located at the same spot.

TABLE 2 - Efficiency of different motor-supply combinations at a fundamental frequency of 50 Hz and 75 Nm

Motor	Mains Supply	IGBT-Inverter		Transistor Inverter
	Sinusoidal	1.2 kHz	12 kHz	1 kHz
SS	87.7 %	85.4 %	86.0 %	84.2 %
RS	87.5 %	84.9 %	85.0 %	84.2 %
RR	86.4 %	84.1 %	84.5 %	83.5 %

TABLE 3 - Temperature (°C) of stator (top) and rotor (bottom)

Motor	Mains Supply	IGBT-Inverter		Transistor Inverter
	Sinusoidal	1.2 kHz	12 kHz	1 kHz
RS	76.7	81.7	76.7	81.2
RR	86.3	88.2	87.3	90.8

Motor	Mains Supply	IGBT-Inverter		Transistor Inverter
	Sinusoidal	1.2 kHz	12 kHz	1 kHz
RS	100	110	104	109
RR	100	103	102	107

The temperature rise in the copper cage motor is higher than in the aluminium cage one, due to the increased losses by the presence of the higher flux density harmonics. However, in the rotor a smaller temperature rise with respect to the stator is noted in the copper rotor, indicating a larger portion of the losses being situated in the stator due to a skin effect free rotor.

5.2. Influence of switching frequency

The higher the chosen switching frequency, the better the spectrum supplied by the inverter. The harmonic currents induced in the motor become smaller. Therefore, losses in the motor decrease. As the losses in the inverter are defined by the number of times the power electronic components have to operate, they increase with a higher switching frequency. It may be expected that an optimum switching frequency exists.

Table 4 shows the losses of the motor with single layer stator winding and standard rotor design, supplied at a fundamental frequency of 50 Hz and loaded with 75 Nm. Table 5 shows the same quantities for the motor with the modified rotor design.

The following conclusions may be drawn from these tables.

- The motor losses are nearly independent of the switching frequency.
- The inverter losses increase with increasing switching frequency.
- For the motor with standard rotor, the overall losses reach a minimum at a switching frequency of 8.4 kHz. For the modified rotor, such an optimum can not be found from the results of the test. This could be due to the fact that in this case measurements are done when the motor has not reached final thermal equilibrium.
- The motor with non-skewed copper rotor bars exhibits higher harmonic losses and lower inverter losses than the motor with skewed aluminium rotor bars at higher switching frequencies.

- The motor losses of the standard motor are smaller than the motor losses of the new motor. This is due to the larger space harmonics in the air gap caused by the lack of skewing.
- With a sinusoidal supply the overall losses are in both cases smaller than when an inverter is used.

TABLE 4 - Losses and efficiency of RS motor at a fundamental frequency of 50 Hz and 75 Nm

f_{switch} [kHz]	Motor losses [kW]	Inverter losses [kW]	Harmonic losses [kW]	Overall losses [kW]	Efficiency [%]
1.2	1.63	0.256	0.118	2.01	85.1
2.7	1.65	0.323	0.063	2.04	84.9
3.6	1.65	0.334	0.057	2.04	84.9
5.4	1.64	0.334	0.046	2.02	85.1
6	1.65	0.341	0.042	2.03	85.0
8.4	1.64	0.284	0.038	1.96	85.4
10.8	1.66	0.366	0.011	2.04	84.9
10	1.64	0.359	0.017	2.02	85.1
11	1.62	0.363	0.032	2.02	85.1
12	1.65	0.376	0.026	2.05	84.9

TABLE 5 - Losses and efficiency of RR motor at a fundamental frequency of 50 Hz and 75 Nm

f_{switch} [kHz]	Motor losses [kW]	Inverter losses [kW]	Harmonic losses [kW]	Overall losses [kW]	Efficiency [%]
1.2	1.82	0.296	0.094	2.21	83.9
2.7	1.82	0.305	0.058	2.19	84.0
3.6	1.82	0.308	0.056	2.18	84.0
5.4	1.81	0.309	0.046	2.17	84.1
6	1.80	0.311	0.048	2.16	84.2
8.4	1.78	0.331	0.042	2.15	84.2
10.8	1.80	0.324	0.040	2.17	84.1
10	1.79	0.332	0.040	2.16	84.1
11	1.76	0.331	0.038	2.13	84.3
12	1.79	0.334	0.038	2.16	84.2

6. Conclusions

The audible noise is influenced both by the inverter switching frequency and the motor construction. At high speeds, the audible noise of the fan dominates and the influence of the switching frequency is rather limited. At lower speeds, a switching frequency of 10 kHz or more leads to values of the audible noise level that are comparable to those found when using a sinusoidal supply. The influence of the flux density space harmonics is much more important. A good winding lay out, skewed rotor bars and closed rotor slots are beneficial for the audible noise level. Improved PWM switching strategies may help to avoid pure tones,

that are particularly found to be disturbing by the human ear, as it is very sensitive to such pure tones.

The motor losses are nearly independent of the switching frequency. The inverter losses, however, increase at higher switching frequencies. The losses depend firmly on the motor construction. All measures taken to reduce the harmonic content of the flux density distribution contribute to loss reduction in a much more pronounced way than the increase of the switching frequency.

The temperature rise of the copper cage motor is higher than of the motor with the aluminium cage. This is due to the increased losses by the presence of the higher flux density harmonics. However, in the rotor a smaller temperature rise with respect to the stator is noted in the copper rotor motor. This indicates that a larger portion of the losses are situated in the stator when using a skin effect free rotor design. This conclusion is very important when dealing with field oriented control drives, where a change in rotor temperature introduces a variation of the rotor time constant, being one of the key parameters of the vector control scheme.

In general, a high switching frequency improves the audible noise and losses, although precautions have to be taken to avoid resonances when looking at the audible noise. The construction of the motor is key, and all measures should be taken to avoid space harmonics in the flux density distribution. The avoidance of space harmonics is more important than the reduction of time harmonics obtained by an increased switching frequency. From the stator and rotor temperature measurements, it can be justified that derating a standard motor at rated speed in the case of state of the art IGBT-frequency-converters is no longer required.

Acknowledgements

The authors are grateful to the Belgian National Fund for Scientific Research (NFWO). The research is also supported by Flanders' Secretary of Economy.

References

- (1) Boglietti, A., Ferraris P., Lazzari M.: Power derating for inverter fed induction motors, Proceedings of the 29th IEEE-IAS Annual Meeting, Oct.2-6 1994, pp. 55-61.
- (2) Chalmers B., Sarkar B.R.; Induction motor losses due to non sinusoidal supply waveforms, Proceeding of the IEE, Part B, vol.115, no.12, 1968, pp. 1777-1782.
- (3) Murphy M.D., Honsinger V.B.: Efficiency optimization of inverter-fed induction motors, Proceedings of the IEEE-IAS Annual Meeting, 1982, pp. 544-552.
- (4) Tomita H., Zheng S.: Optimal efficiency control for energy saving of variable speed ac motor, EPE 1989, pp. 819-822.
- (5) Kirschen D.S., Novotny D.W., Surwanwisoot W.: Minimizing induction motor losses by excitation control in variable frequency drives, IEEE Trans.Vol.IA-20, no.5, Sept./Oct. 1984., pp. 1244-1250.

- (6) Lajoie-Mazenc E., Pratmarty D.: Etat de l'offre européenne de convertisseurs de fréquence pour machines asynchrones, Electricité de France, Direction des Etudes et Recherches, Mars 1993.
- (7) Malfait A., Reekmans R., Belmans R.: Audible noise and losses in variable speed induction motor drives with IGBT-inverters, 29th Annual Meeting IEEE-IAS, 1994, 2-6 Oct., Vol.I, pp.693-700.
- (8) Belmans R., Verdyck D., Geysen W., Findlay R.: Electromechanical analysis of the audible noise of an inverter fed squirrel cage induction motor, IEEE Transactions on Industry Applications, Vol.27, No.3, May/June 1991, pp. 539-544.
- (9) Belmans R., Geysen W., Bailly G., Sattler P-K.: Theoretical and experimental analysis of the audible noise of an inverter fed squirrel cage induction motor, International Conference on Electrical Machines ICEM-90, August 13-15 1990, pp. 485-490.
- (10) Muster J., Budig P.K., Belmans R., Geysen W.: Audible noise in speed-controlled inverter-fed medium-sized induction motors, ETEP, vol.5, no.1, Jan/Febr. 1995, pp. 5-13.
- (11) Verdyck D., Belmans R.: A vibrational modal using modal shapes and magnetic forces: experimental results for permanent magnet machine, Archiv für Elektrotechnik 77, 1994, pp. 383-389
- (12) Verdyck D., Belmans R.: An acoustic model for a permanent magnet machine: modal shapes and magnetic forces, IEEE Transactions on industry applications, vol.30, no.6, 1994, pp. 1625-1631

Fig. 1: Different motor-supply combinations

Fig. 2: Lay-out of the experimental set-up

Fig. 3: Overall audible noise level of the standard motor (top) and the single layer wind stator (bottom) as a function of the inverter switching frequency at different fundamental frequencies and a load torque of 60 Nm.

Fig. 4: Audible noise spectrum of HS motor with 50 Hz sinusoidal and 50 Hz transistor inverter supply (switching frequency 1 kHz)

Fig. 5: Voltage and audible noise spectrum of HS motor with IGBT-inverter supply (12 kHz)

Fig. 6: Voltage and audible noise spectrum of HS motor with IGBT-inverter supply (11 kHz)

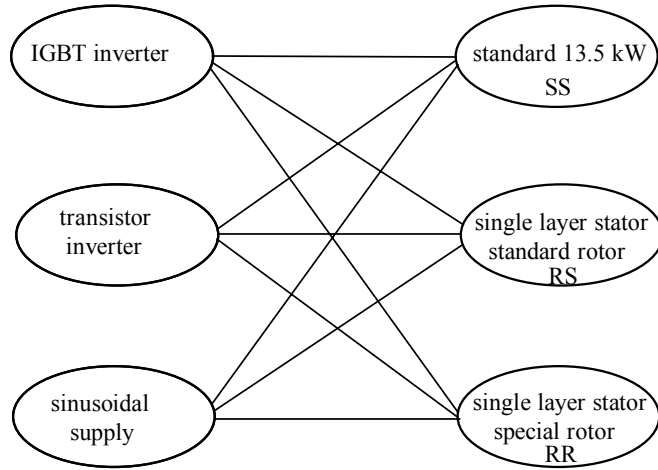


Fig. 1: Different motor-supply combinations

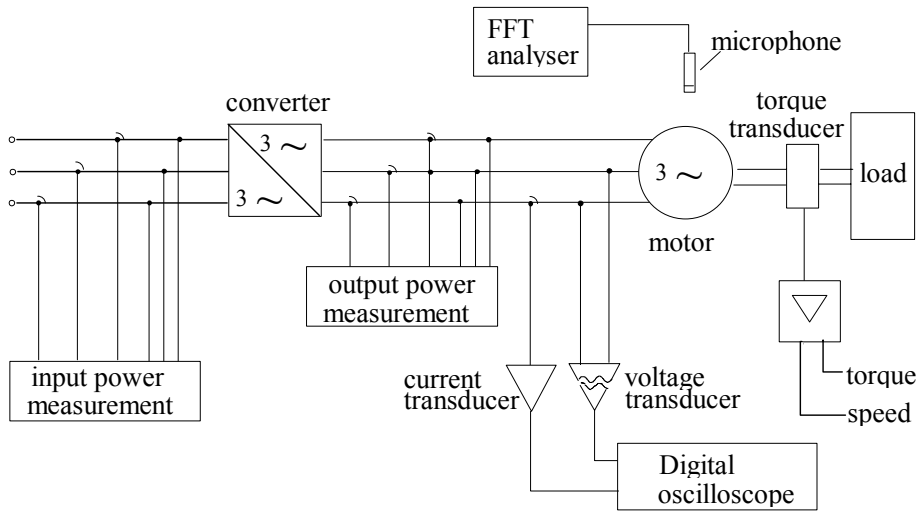


Fig. 2: Lay-out of the experimental set-up

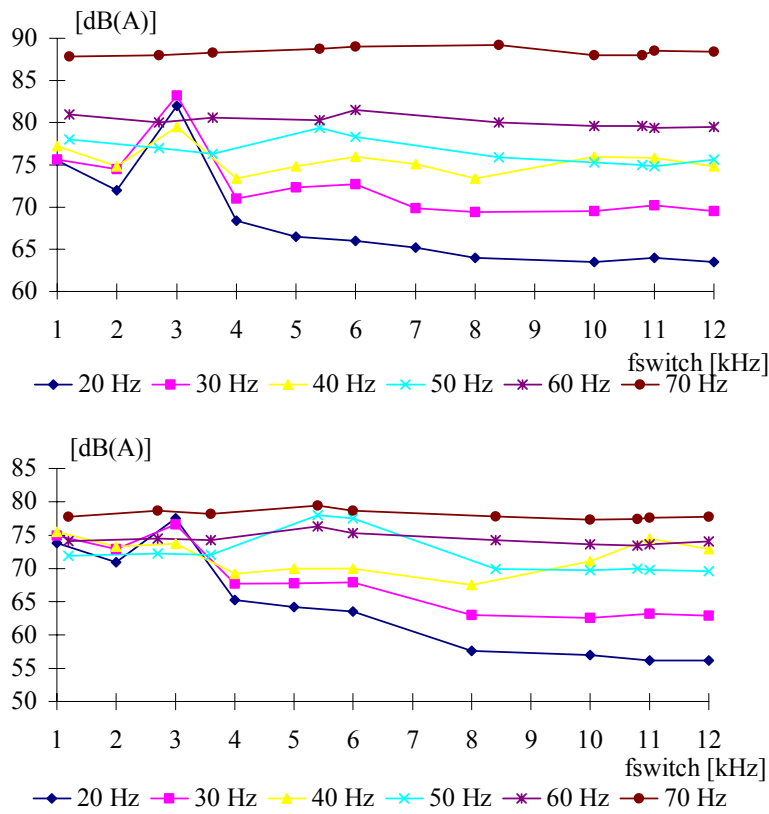


Fig. 3: Overall audible noise level of the standard motor (top) and the single layer wind stator (bottom) as a function of the inverter switching frequency at a load torque of 60 Nm and at different fundamental frequencies as indicated by the labels at the bottom of the figure.

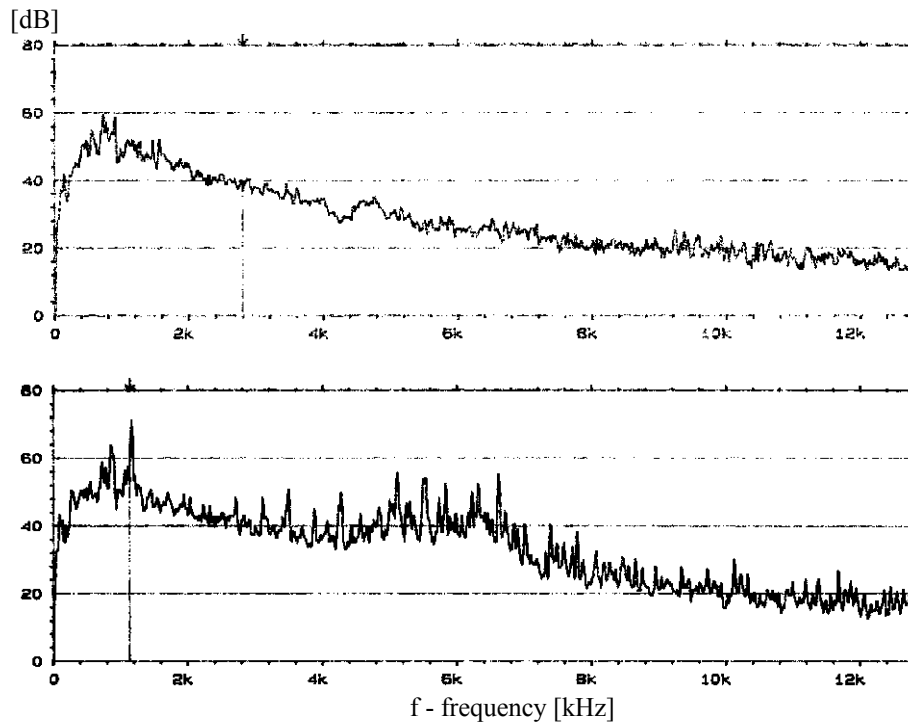


Fig. 4: Audible noise spectrum of RS motor with 50 Hz sinusoidal and 50 Hz transistor inverter supply (switching frequency 1 kHz)

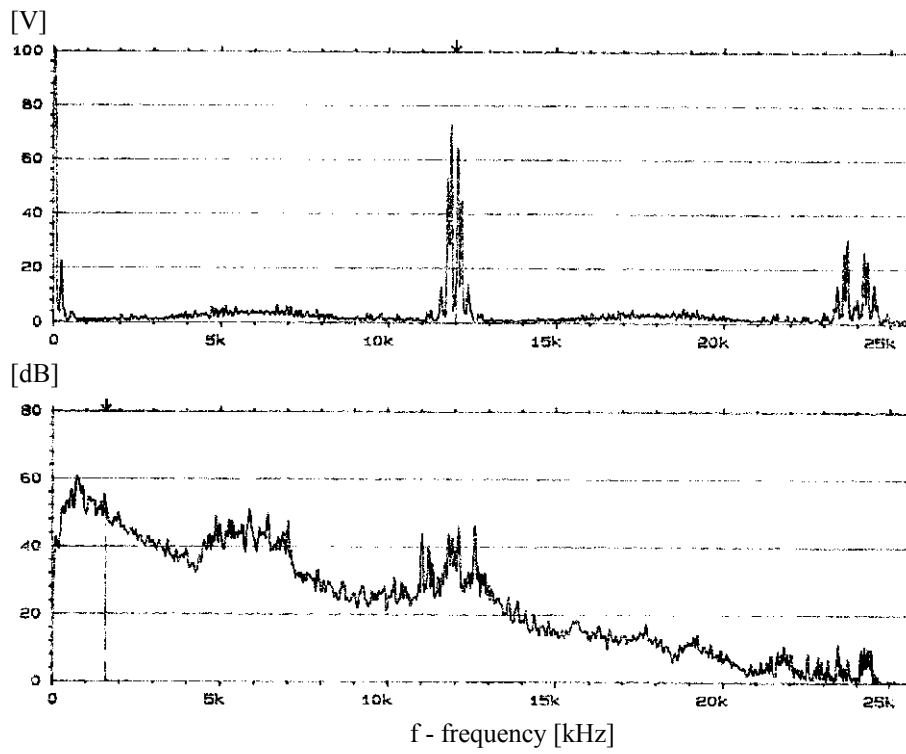


Fig. 5: Voltage and audible noise spectrum of RS motor with IGBT-inverter supply (12 kHz)

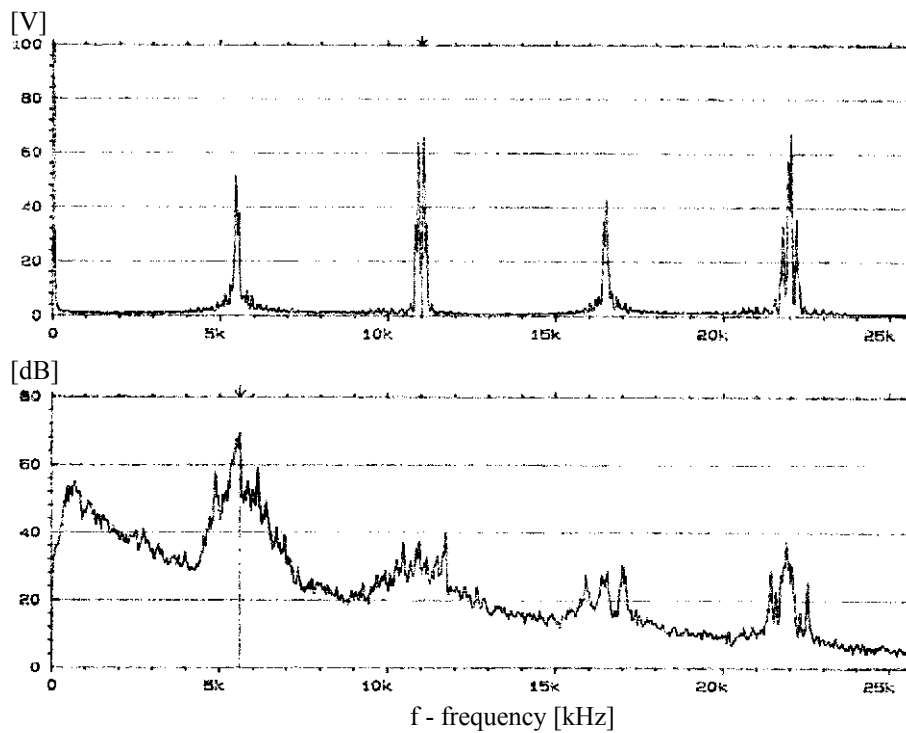


Fig 6: Voltage and audible noise spectrum of RS motor with IGBT-inverter supply (11 kHz)